Transport in nonhomogeneous media: from modeling to control with Lyapunov techniques, part I

Emmanuel WITRANT[1]

In collaboration with:

[1]UJF / GIPSA-lab (Control Systems Department), Grenoble, France.
ACCESS Linnaeus Center/Alfvèn-lab, KTH, Stockholm, Sweden.
Association EURATOM-CEA, CEA/DSM/IRFM, Cadarache
Laboratoire de Glaciologie et Géophysique de l'Environnement, Grenoble, France.
ABB, L2S/Suplec, CERN, Boliden, IIT, UAQ, UNISI.

33th Int. Sum. School of Auto. Control Grenoble, Sept 12, 2012

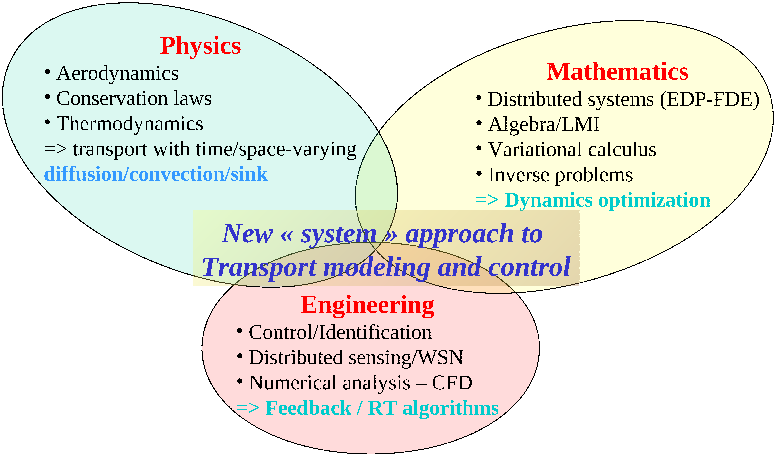

$$\frac{\partial \zeta}{\partial t} + \nabla \cdot \mathcal{A}(\zeta, \mathbf{x}, t) + \nabla \mathcal{D}(\nabla \cdot \zeta, \zeta, \mathbf{x}, t) = \mathcal{S}_o(u, \mathbf{x}, t) - \mathcal{S}_i(\zeta, \mathbf{x}, t)$$

$$y = g(\zeta, \mathbf{x}, t)$$

Applications

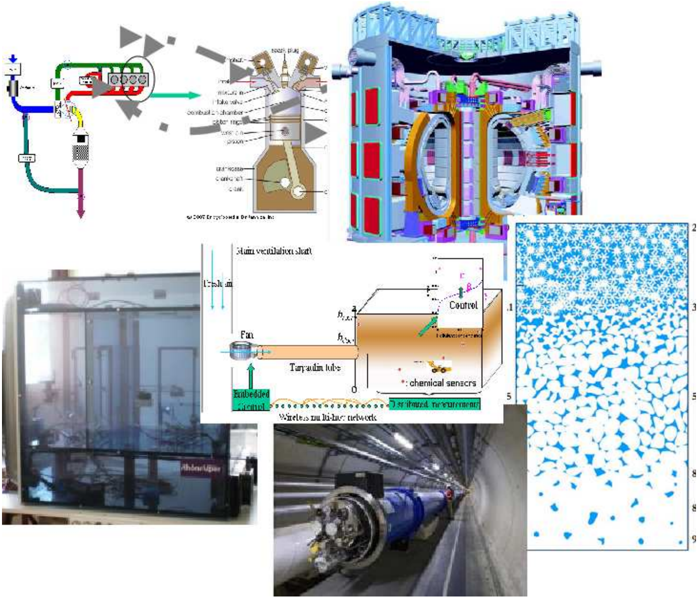

Advective transport

$$\frac{\partial \zeta}{\partial t} + \nabla \cdot \mathcal{A}(\zeta, \mathbf{x}, t) + \nabla \mathcal{D}(\nabla \cdot \zeta, \zeta, \mathbf{x}, t) = \mathcal{S}_o(u, \mathbf{x}, t) - \mathcal{S}_i(\zeta, \mathbf{x}, t)$$

- Focus on the "traveling effect", i.e. Telegrapher's equation
- No shock wave, or just the energy loss effect
- i.e. continuity if velocity independ. on density gradient:
  - mass can be neither created or destroyed in finite space
    $$\frac{\partial}{\partial t} \oint_{\mathcal{V}} \rho d\mathcal{V} + \oint_S \rho \mathbf{V} \cdot \mathbf{dS} = 0$$

  $\Rightarrow$ at a point in the flow (continuum hyp.): $\frac{\partial \rho}{\partial t} + \nabla \cdot (\rho \mathbf{V}) = 0$

$\longrightarrow$ Space-invariant parameters (volume-averaged transport/communication in NCS)

$\longrightarrow$ Travelling waves (Euler/Navier-Stokes)

$\longrightarrow$ Complex combinations (MHD)

Mining potential wireless control architecture [IJRNC'10]

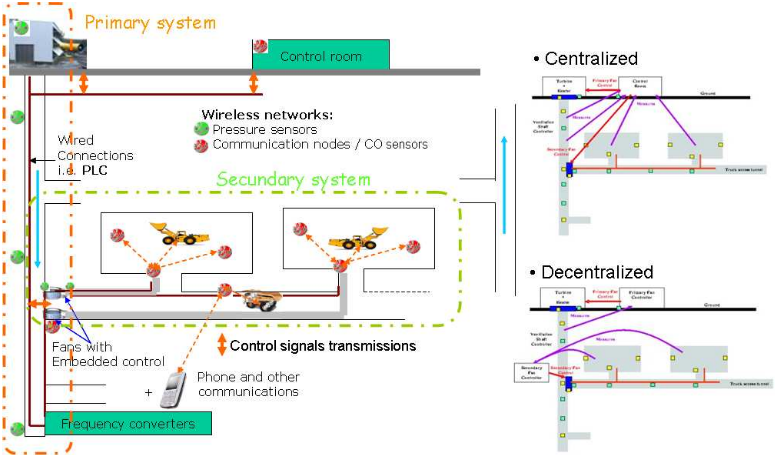

Space-invariant parameters

Suppose that we can express the transport equation as:

$$\frac{\partial \zeta}{\partial t} + \mathcal{A}_1(\zeta, \mathbf{x}, t)\nabla\zeta + \mathcal{D}_1(\nabla\cdot\zeta, \zeta, \mathbf{x}, t)\nabla^2\zeta + \mathcal{S}_{i,1}(\zeta, \mathbf{x}, t)\zeta = \mathcal{S}_{o,1}(u, \mathbf{x}, t)u$$

If the flow is "mostly unidirectional" in x and "sufficiently quasi-steady", then we can use volume averaging to get the "LPV" representation:

$$\frac{\partial \zeta}{\partial t} + \bar{\mathcal{A}}_1(t)\frac{\partial \zeta}{\partial x} + \bar{\mathcal{D}}_1(t)\frac{\partial^2 \zeta}{\partial x^2} + \bar{\mathcal{S}}_{i,1}(t)\zeta = \bar{\mathcal{S}}_{o,1}(t)u$$

where $\bar{\mathcal{X}} \doteq \oint_{\mathcal{V}} \mathcal{X} d\mathcal{V}$.

$\Rightarrow$ Given (distributed) measurements, estimate transport coefficients and set feedback using ζ or $y = g(\zeta, x, t)$

Mine pressure model [Ieee CASE'08]

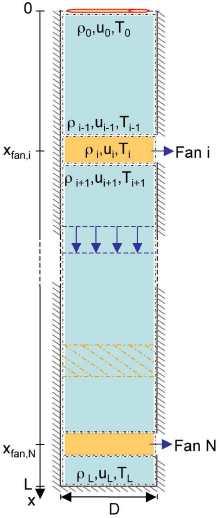

Starting from Euler equations

$$\frac{\partial}{\partial t}\begin{bmatrix}\rho \\ \mathbf{M} \\ \rho E\end{bmatrix} + \nabla\cdot\begin{bmatrix}\mathbf{M} \\ \mathbf{M}^T\otimes\mathbf{V}+p\mathbf{I} \\ \mathbf{M}H\end{bmatrix} = \begin{bmatrix}0 \\ 0 \\ \dot{q}\end{bmatrix},$$

Hypotheses

1. only static pressure considered in energy conservation;
2. impulsive term $\ll$ compared to pressure in momentum conservation;
3. **M** simplified using Saint-Venant equations $\rightarrow$ algebraic relationship.

Give the pressure model (ρ and M averaging)

$$\frac{\partial p}{\partial t} = -\frac{\partial}{\partial x}\left[\frac{M}{\rho}\cdot\left(1+\frac{R}{c_v}\right)p\right] + \frac{R}{c_v}\dot{q}$$

Online LPV parameter estimation [W, Marchand'08]

i.e. $\vartheta(t) = \{\bar{\mathcal{A}}_1(t),\ \bar{\mathcal{D}}_1(t),\ \bar{\mathcal{S}}_{i,1}(t),\ \bar{\mathcal{S}}_{o,1}(t)\}$

Theorem (parameter estimation for affine PDE):

Consider the class of systems

$$\begin{cases} \zeta_t = \mathcal{F}(\zeta, \zeta_x, \zeta_{xx}, u, \vartheta)\vartheta \\ a_1\zeta_x(0,t) + a_2\zeta(0,t) = a_3 \\ a_4\zeta_x(L,t) + a_5\zeta(L,t) = a_6 \end{cases}$$

with distributed measurements of $\zeta(x,t)$ and for which we want to estimate ϑ. Then

$$\|\zeta(x,t) - \hat{\zeta}(x,t)\|_2^2 = e^{-2(\gamma+\lambda)t}\|\zeta(x,0) - \hat{\zeta}(x,0)\|_2^2$$

if

$$\begin{cases} \hat{\zeta}_t = \mathcal{F}(\hat{\zeta}, \hat{\zeta}_x, \hat{\zeta}_{xx}, u, \hat{\vartheta})\hat{\vartheta} + \gamma(\zeta - \hat{\zeta}) \\ a_1\hat{\zeta}_x(0,t) + a_2\hat{\zeta}(0,t) = a_3 \\ a_4\hat{\zeta}_x(L,t) + a_5\hat{\zeta}(L,t) = a_6 \\ \dot{\hat{\vartheta}} = \mathcal{F}(\hat{\zeta}, \hat{\zeta}_x, \hat{\zeta}_{xx}, u, \hat{\vartheta})^\dagger[\zeta_t + \lambda(\zeta - \hat{\zeta})] \end{cases}$$

Ex.: comparison with gradient-descent algorithm

$$p_t = d(t)p_{xx} + c(t)p_x + r(t)p + s(t)p_{ext}(x,t)$$

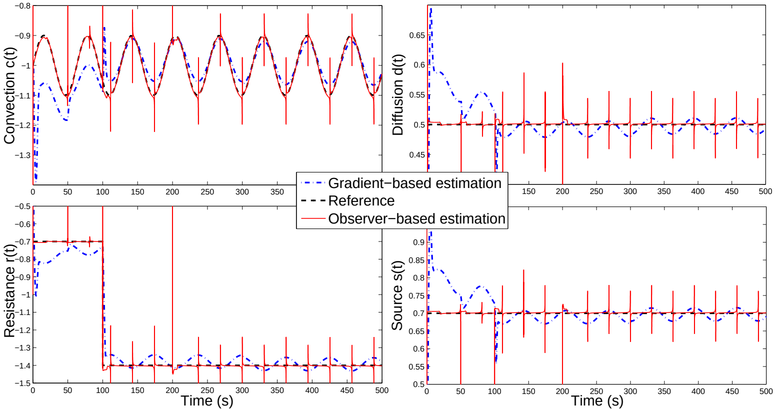

⇒ very accurate results, need to add a filter.

Time-delay model [W, Niculescu'10]

Consider the advective-resistive flow:

$$\zeta_t(x,t) + \bar{\mathcal{A}}_1(t)\zeta_x(x,t) = -\bar{\mathcal{S}}_{i,1}(t)\zeta(x,t)$$

with $\zeta(0,t) = u(t)$, $\zeta(x,0) = \psi(x)$. Applying the method of characteristics with the new independent variable θ as

$$\zeta(\theta) \doteq \zeta(x(\theta), t(\theta))$$

It follows that (solution including time axis)

$$\zeta(L,t) \doteq u(t-\theta_f) exp\left(-\int_0^{\theta_f} \bar{\mathcal{S}}_{i,1}(\eta)d\eta\right), \text{ with } L = \int_{t-\theta_f}^{t} \bar{\mathcal{A}}_1(\eta)d\eta$$

The average state $\bar{\zeta}(t) \doteq \int_0^L \zeta(\eta,t)d\eta$ is provided by the Delay Differential Equation

$$\frac{d}{dt}\bar{\zeta} = \bar{\mathcal{A}}_1(t)\left[u(t) - u(t-\theta_f) exp\left(-\int_0^{\theta_f} \bar{\mathcal{S}}_{i,1}(\eta)d\eta\right)\right] - \bar{\mathcal{S}}_{i,1}(t)\bar{\zeta}$$

Tracking feedback controller design

Design a feedback such that the average distributed pressure:

$$\bar{\zeta}(t) = \frac{1}{L}\int_0^L \zeta(x,t)dx$$

tracks reference $\bar{\zeta}_r(t)$. Achieved if (fixed point theorem):

$$\dot{\bar{\zeta}}(t) - \dot{\bar{\zeta}}_r(t) + \lambda(\bar{\zeta}(t) - \bar{\zeta}_r(t)) = 0$$

Using the previous DDE and solving for $u(t)$, it follows that

$$\frac{d}{dt}\bar{\zeta} = L\bar{\mathcal{A}}_1(t)\left[u(t) - u(t-\theta_f)exp\left(-\int_0^{\theta_f}\bar{\mathcal{S}}_{i,1}(\eta)d\eta\right)\right] - \bar{\mathcal{S}}_{i,1}(t)\bar{\zeta}$$

$$u(t) = -\frac{L}{\bar{\mathcal{A}}_1(t)}\left[-\bar{\mathcal{S}}_{i,1}(t)\bar{\zeta}(t) + \lambda(\bar{\zeta}(t) - \bar{\zeta}_r)\right] + \zeta(L,t)$$

ensures

$$|\bar{\zeta}(t) - \bar{\zeta}_r| = |\bar{\zeta}(0) - \bar{\zeta}_r|e^{-\lambda t}$$

Mine reference model

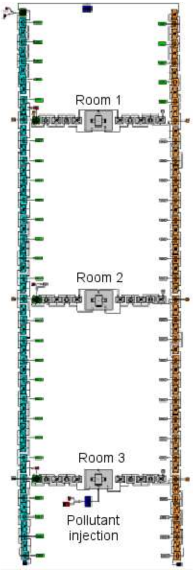

Simulator properties:

- ventilation shafts ≈ 28 control volumes (CV), 3 extraction levels
- regulation of the turbine and fans
- flows, pressures and temperatures measured in each CV
- Computation time 34× faster than real-time

Case study:

- 1^{st} level fan not used (natural airflow), 2^{nd} operated at 1000 s (150 rpm) and 3^{rd} runs continuously (200 rpm)
- CO pollution injected in 3^{rd} level
- measurement of flow speed, pressure, temperature and pollution at the surface and extraction levels

feedback control results for mine ventilation

Reference and effective turbine output pressure:

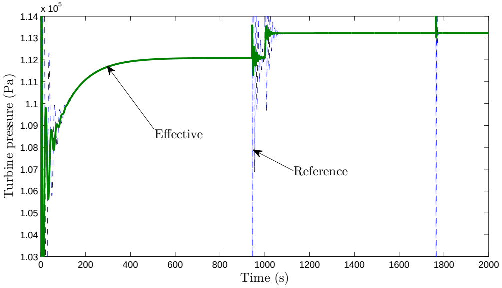

Feedback tracking error:

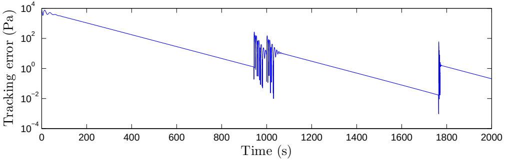

⇒ Sensible to initial conditions and some numerical integration errors but exponential convergence verified!

Information transport

Physical models

- Telegrapher's equation (homogeneous if $\alpha = 0$):

$$\begin{bmatrix} V_t \\ I_t \end{bmatrix} + \begin{bmatrix} 0 & 1/C \\ 1/L & 0 \end{bmatrix} \begin{bmatrix} V_z \\ I_z \end{bmatrix} = \alpha(t) \frac{VI}{2} \begin{bmatrix} 0 & -1/C \\ 1/L & 0 \end{bmatrix} \begin{bmatrix} V \\ I \end{bmatrix}$$

- Local inductance and capacitance variations captured with $\alpha(t)$ in the elementary cell [Ph.D.'05]:

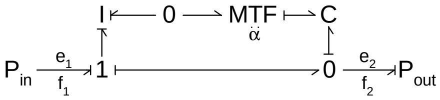

induce wave reflections and time-varying delays.

Communication models

I.e. Fluid-flow model for the network [Misra et al. 2000, Hollot and Chait 2001]: TCP with proportional active queue management (AQM) set the window size W and queue length q variations as

$$\begin{aligned}\frac{dW_i(t)}{dt} &= \frac{1}{R_i(t)} - \frac{W_i(t)}{2}\frac{W_i(t-R_i(t))}{R_i(t-R_i(t))}p_i(t),\\ \frac{dq(t)}{dt} &= -C_r + \sum_{i=1}^{N}\frac{W_i(t)}{R_i(t)}, \quad q(t_0) = q_0,\end{aligned}$$

where $R_i(t) \doteq \dfrac{q(t)}{C_r} + T_{pi}$ is the round trip time, C_r the link capacity, $p_i(t) = K_p q(t - R_i(t))$ the packet discard function and T_{pi} the constant propagation delay. The average time-delay is $\tau_i = \frac{1}{2}R_i(t)$

Wireless Sensor Networks

[Park, di Marco, Soldati, Fischione, Johansson'09...]

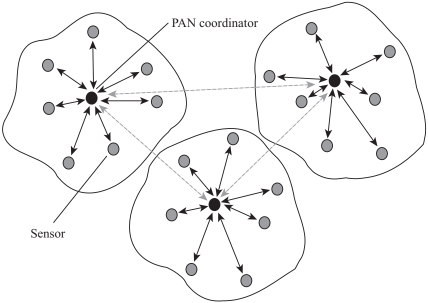

- IEEE 802.15.4, Markov chain model, network & control codesign
- Communication constraints = time-delay + packet loss

Delays characterization [Springer'10]

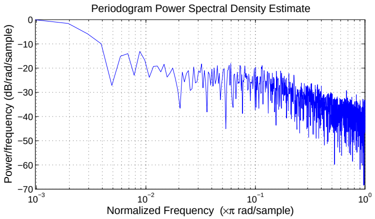

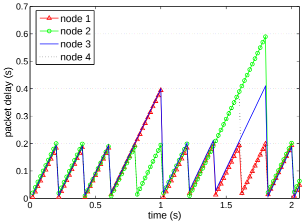

- Three-frequencies jitter & KUMSUM Kalman estimation
- Synchronous/async. cases
- Packet losses as time-delays

Feedback design

I.e. finite-spectrum assignment with online adaptation of the horizon of a MPC feedback scheme with robust gain design [TAC'07]

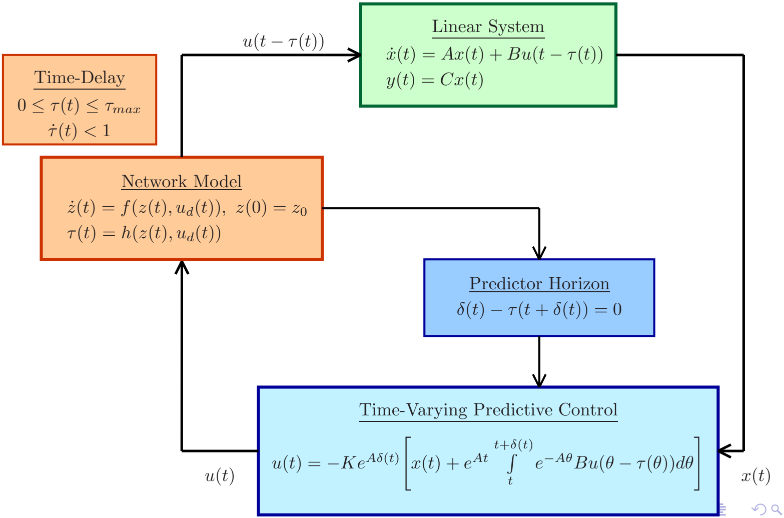

Experimental results on an inverted pendulum

Control over a network with 2 users (LQR gain design):

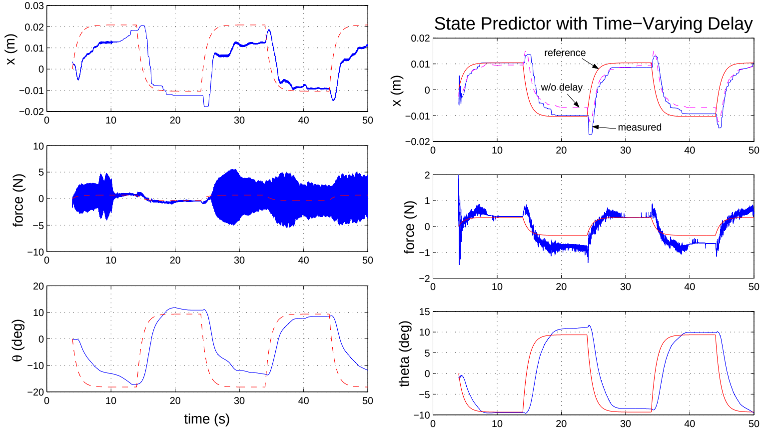

(a) Predictor with fixed horizon.

(b) with time-varying horizon.

Room temperature control over multi-hop WSN in intelligent buildings [TdS'09]

$$\frac{dx}{dt} = (A_1 + A_2(u))x + (B_1 + B_2(u))u + B_w w + P\mathcal{P}(x - Ux) + s + \mathcal{H}(Y, x)$$

Simulation results [IMA'10]

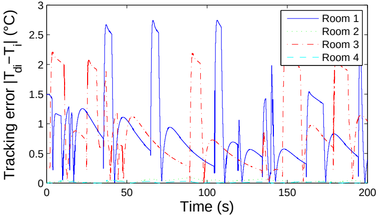

(c) Synchronous mode (Mixed-sensitivity H_∞)

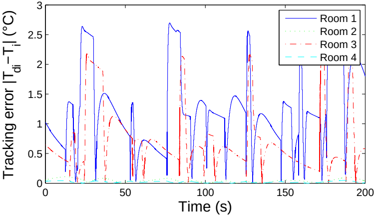

(d) Asynchronous mode (Mixed-sensitivity H_∞)

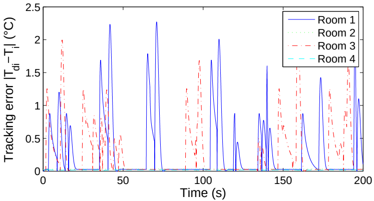

(e) BRL with weights, post check for TD stability (Skelton et al., 1997)

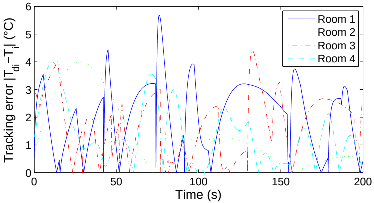

(f) Delay constraint during the design (Seuret, 2009)

Travelling waves modeling

The conservative form of Euler equations:

$$\frac{\partial}{\partial t}\begin{bmatrix}\rho\\ \vec{M}\\ E\end{bmatrix}+\vec{\nabla}\cdot\begin{bmatrix}\rho\cdot\vec{V}\\ \rho\cdot\vec{V}^T\otimes\vec{V}+P\cdot I\\ \rho\cdot\vec{V}\cdot\left(u+\frac{P}{\rho}\right)\end{bmatrix}=\begin{bmatrix}0\\0\\q\end{bmatrix}$$

writes in 1-D for a straight line topology and neglecting the kinetic effects (V^2) as:

$$\frac{\partial\zeta}{\partial t}+\mathcal{A}_1(\zeta,\mathbf{x},t)\nabla\zeta=u$$

where $\zeta=[\ \rho\quad M\quad E\ ]^T$, $u=[\ 0\quad 0\quad q\ ]^T$ and $\mathcal{A}_1$ is the Jacobian flux matrix [Hirsh'90] (ideal gas hyp.):

$$\mathcal{A}_1=\begin{bmatrix}0 & 1 & 0\\ \frac{(\gamma-3)V^2}{2} & (3-\gamma)V & \hat{\gamma}\\ \hat{\gamma}V^3-\frac{\gamma VE}{\rho} & \frac{\gamma E}{\rho}-\frac{3\hat{\gamma}V^2}{2} & \gamma V\end{bmatrix}$$

Decoupled model

- The eigenvalues of the Jacobian define the traveling waves, going into two directions: $\lambda_1(\zeta) = V - c$, $\lambda_2(\zeta) = V$ and $\lambda_3(\zeta) = V + c$
- Using a change of coordinates $\bar{\zeta}$ given by the Riemann invariants, we obtain a quasi-linear hyperbolic formulation with (isentropic case):

$$\mathcal{A}_1 = \begin{bmatrix} \lambda_1(\bar{\zeta}) & 0 & 0 \\ 0 & \lambda_2(\bar{\zeta}) & 0 \\ 0 & 0 & \lambda_3(\bar{\zeta}) \end{bmatrix}$$

Cryogenics at CERN [Cryogenics'10]

LHC sector 5-6 with the main cooling loops for the superconducting magnets:

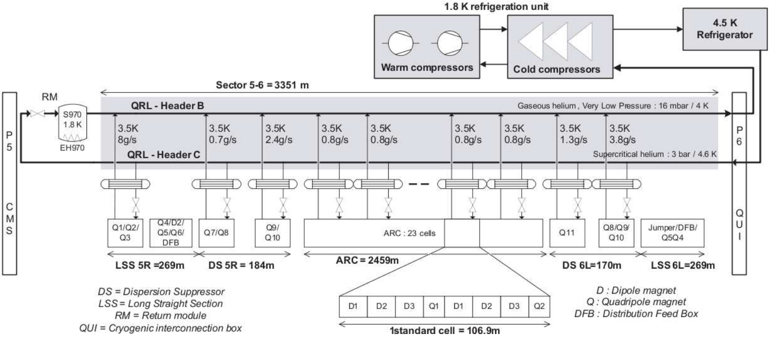

Temperature transport

Impact of convection heat, hydrostatic pressure and friction pressure drops:

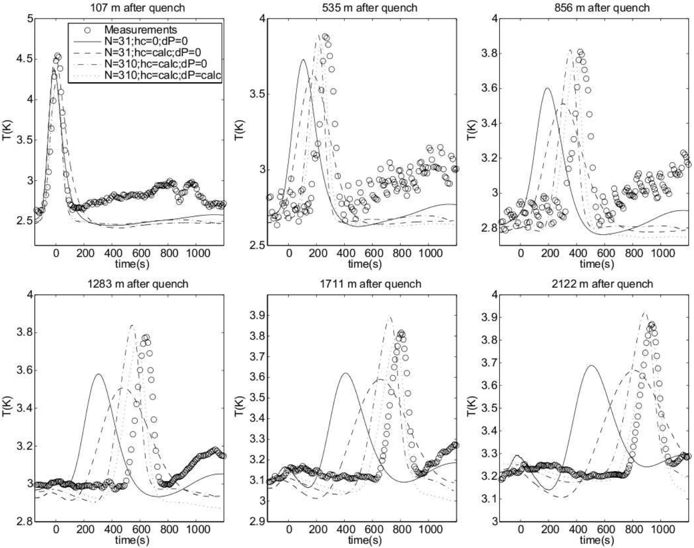

Complex models

Resistive-wall mode physics in RFP:

from Magnetohydrodynamic instability to perturbed ODE

- Linear stability investigated by periodic spectral decomposition

$$\mathbf{b}(r,t) = \sum_{mn} \mathbf{b}_{mn}(r) e^{j(t\omega + m\theta + n\phi)}$$

Fourier eigenmodes $\mathbf{b}_{mn}(r)$ with growth-rate $\gamma_{mn} = j\omega_{mn}$,

- Ideal MHD modes:

$$\tau_{mn}\dot{b}^r_{mn} - \tau_{mn}\gamma_{mn} b^r_{mn} = b^{r,ext}_{mn}$$

b^r_{mn}: radial component of perturbed field, $b^{r,ext}_{mn}$: external active coil, τ_{mn}: penetration time.

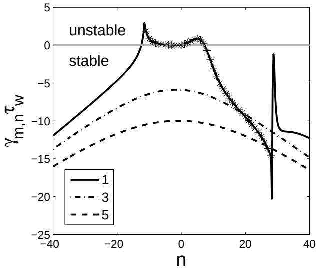

Growth-rates $\tau_w\gamma_{mn}$. *: Integer-n non-resonant positions (RWMs) for $m = 1$.

Stability analysis and delay effects [CDC'08, IOP PPCF'10]

Closed-loop dynamics with multiple delays and time-scales:

- Infinite spectrum of the Delay Differential Equation

$$\det \Delta(s) = \det\left(sI - \mathcal{A}_0 - \sum_{i=1}^{n} \mathcal{A}_i e^{-s\tau_i}\right) = 0$$

- Mode-control and perfect decoupling: SISO dynamics (fixed gains)

$$G_{mn}(s) = \frac{1}{\tau_{mn}s - \tau_{mn}\gamma_{mn}} \frac{1}{\tau_c s + 1} \frac{1}{\tau_a s + 1} e^{-s\tau_h}$$

→ fictitious but useful for disturbance rejection and resonant-field amplification analysis

Controlled thermonuclear fusion

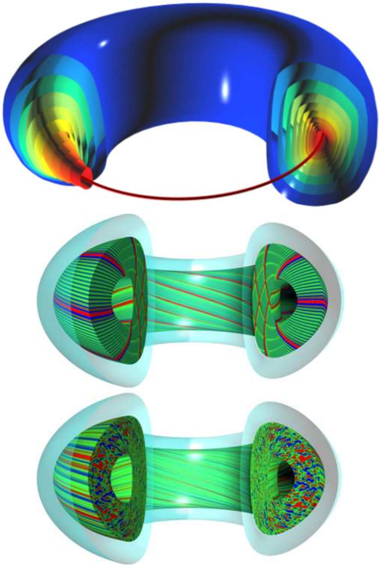

Tokamak:

- Sustainable nuclear energy
- Magnetic confinement and RF actuation plasma self heating

Plasma Physics Issues:

- MHD Stability
- Control of Plasma Purity
- Heat Confinement
- Steady State Operation
- Plasma self heating using α-particles

Experimental results

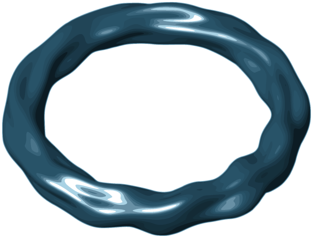

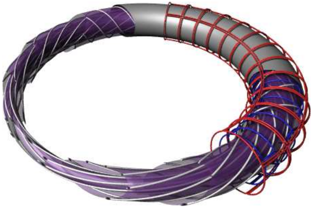

- Direct Eigenvalue Optimization
- Two different parameterizations, implicitly assigning the closed-loop performance and control-input norm
- Robust: convergence within 10 – 30 iterations

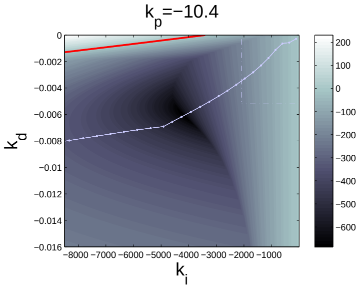

$\Rightarrow$ *44 % reduction of average field energy at the expense of higher input power* (+28 %).

Preliminary conclusions

- Time-delay is often the main issue
- Its proper inclusion in the feedback architecture compensates advection and losses can be dealt with an integral action
- Information transport strongly affected by information losses and needs robustness
- Capturing the traveling wave requires finer modeling
- Strong relationship with CFD
- Adapt model complexity to measurements sparsity

Diffusive transport

$$\frac{\partial \zeta}{\partial t} + \nabla \cdot \mathcal{A}(\zeta, \mathbf{x}, t) + \nabla \mathcal{D}(\nabla \cdot \zeta, \zeta, \mathbf{x}, t) = \mathcal{S}_o(u, \mathbf{x}, t) - \mathcal{S}_i(\zeta, \mathbf{x}, t)$$

$$y = g(\zeta, \mathbf{x}, t)$$

- Inherent stability
- Performance and robustness issues
- Addapt the model complexity to capture I/O map
- Real-time modeling objective

Quasi-steady state (QSS) behavior

Consider again the simplified transport model:

$$\frac{\partial \zeta}{\partial t} + \bar{\mathcal{D}}_1(t') \frac{\partial^2 \zeta}{\partial x^2} = \bar{\mathcal{S}}_{o,1}(x,t') - \bar{\mathcal{S}}_{i,1}(t')\zeta$$

$$\frac{\partial \zeta}{\partial x}(0,t) = 0, \quad \zeta(1,t) = \zeta_L(t')$$

where ζ reacts "sufficiently quickly" to the slow variations in t'. t' then considered as constant and ζ approximated by the steady-state behavior $\tilde{\zeta}_{qss}(x)$:

$$\begin{cases} \bar{\mathcal{D}}_1 \, \tilde{\zeta}_{qss,xx} + \bar{\mathcal{S}}_{i,1} \, \tilde{\zeta}_{qss} - \bar{\mathcal{S}}_{o,1} = 0, \rightarrow \text{ no time-derivative!} \\ \tilde{\zeta}_{qss,x}(0) = 0, \quad \tilde{\zeta}_{qss}(1) = \tilde{\zeta}_L. \end{cases}$$

Solving QSS [CDC'09]

- QSS behavior given by:

$$
\begin{aligned}
\tilde{\zeta}_{qss}(x,t') &= \frac{\tilde{\zeta}_L - \mathcal{C}(\bar{\mathcal{S}}_{o,1})}{\cosh\lambda}\cosh\lambda x \\
&\quad + \frac{1}{\sqrt{\bar{\mathcal{D}}_1\bar{\mathcal{S}}_{i,1}}}\int_0^x \sinh[\lambda(\eta - x)]\bar{\mathcal{S}}_{o,1}(\eta,t')d\eta, \\
\mathcal{C}(\bar{\mathcal{S}}_{o,1}) &\doteq \frac{1}{\sqrt{\bar{\mathcal{D}}_1\bar{\mathcal{S}}_{i,1}}}\int_0^1 \sinh[\lambda(\eta-1)]\bar{\mathcal{S}}_{o,1}(\eta,t')d\eta
\end{aligned}
$$

with $\lambda = -\sqrt{\bar{\mathcal{S}}_{i,1}/\bar{\mathcal{D}}_1}$.

- Approximation error $z(x,t) \doteq \zeta(x,t) - \tilde{\zeta}_{qss}(x,t)$ obeys

$$\|z(x,t)\|_2^2 \leq e^{-\frac{-\bar{\mathcal{D}}_1+4\bar{\mathcal{S}}_{i,1}}{2}t}\|z(x,0)\|_2^2.$$

$\Rightarrow$ First order response that can be used to verify the order of magnitude of $-\bar{\mathcal{D}}_1 + 4\bar{\mathcal{S}}_{i,1}$.

Identifying density sources in the Scrape-off layer

- Scrape-off layer (SOL): between the last closed magnetic surface (*separatrix*) and the wall;
- LH (RF current drive) efficiency strongly depends on the electron density the SOL.

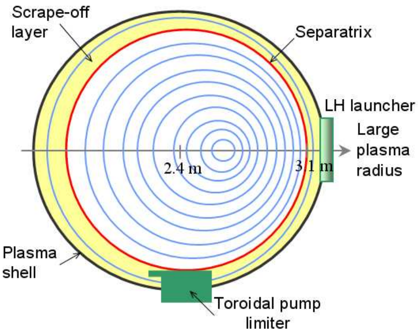

Problem formulation (linearizing and averaging):

$$\frac{\partial \tilde{n}}{\partial t} = D_\perp(t)\frac{\partial^2 \tilde{n}}{\partial r^2} - \frac{c_s(t)}{2L_c(t)}\tilde{n} + S(r,t)$$

$$\frac{\partial \tilde{n}(0,t)}{\partial r} = 0, \; \tilde{n}(L,t) = \tilde{n}_L(t)$$

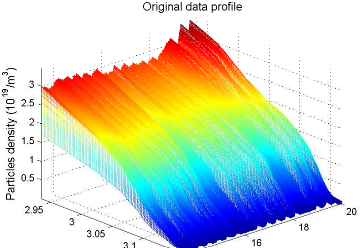

Optimal source tracking for the LTI discretized model

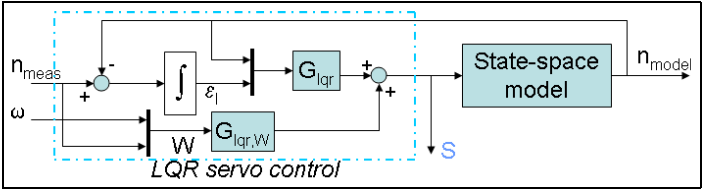

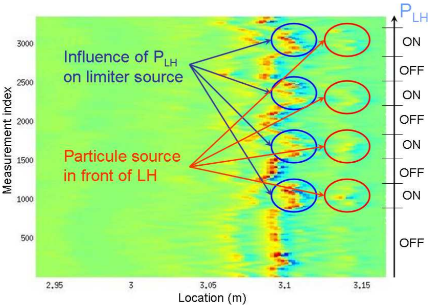

- Satisfying accuracy ($\epsilon_I < 5\ \% n_e$)
- Reveals the influence of LH power as:
  - ★ amplification + shift of limiter source;
  - ★ smaller source in front of LH.

⇒ Validates of LH as a source term in the model.

- BUT unconstrained (negative S terms) and not explicitly related to physical model.

Shape identification with QSS

- Shape hypothesis:

$$S(x,t') \approx \sum_{i=l,\,LH} \vartheta_i(t') e^{\beta(x,\mu_i(t'),\sigma_i(t'))},$$

where ϑ_i = amplitude, $\beta(\cdot)$ = dilatation function, σ_i = dilatation coefficient and μ_i = translation.

- Identified parameters $\theta(t') \doteq \{\vartheta_l,\, \mu_l,\, \sigma_l,\, \vartheta_{LH},\, \mu_{LH},\, \sigma_{LH}\}$ obtained by solving:

$$\min_\theta \left\{ J(\theta,\, t') = \frac{1}{2}\int_0^1 (\tilde{n}_{meas}(x,t') - \tilde{n}_{qss}(x,\theta,t'))^2 dx \right\}$$

for each sampling instant t'.

$\Rightarrow$ Nonlinear optimization problem with analytical gradient computation

Experimental results

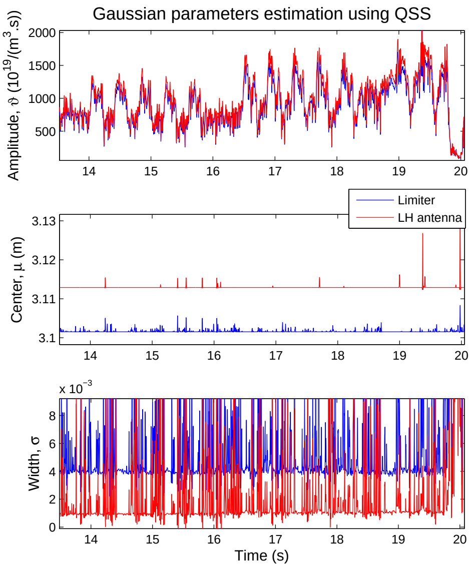

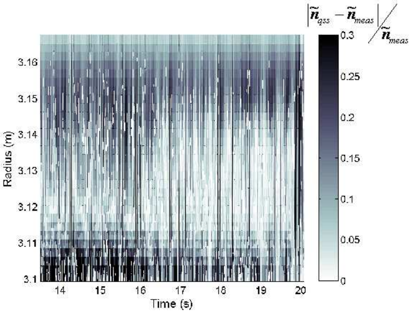

Satisfying estimation, with some limitations:

- parameter decoupling
- underestimated LH location
- noisy width

Dynamics and peripheral components

$$\frac{\partial \zeta}{\partial t} + \nabla \cdot \mathcal{A}(\zeta, \mathbf{x}, t) + \nabla \mathcal{D}(\nabla \cdot \zeta, \zeta, \mathbf{x}, t)$$
$$= \mathcal{S}_o(u, \mathbf{x}, t) - \mathcal{S}_i(\zeta, \mathbf{x}, t)$$
$$y = g(\zeta, \mathbf{x}, t)$$

For sufficiently deterministic transport, improve the accuracy of I/O map by getting the proper approximation of peripheral components.

Key issues:

- time-variations of the transport coefficient
- nonlinear components
- “simple” model of the distributed inputs

Poloidal flux dynamics in a tokamak

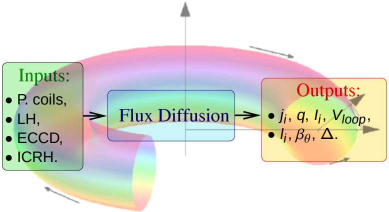

Hypotheses (Tore Supra):

- cylindrical coordinates (neglect GSS),
- neglect diamagnetic effect,

System dynamics [Blum'89, Brégeon & al'98]:

$$\frac{\partial \psi_x}{\partial t}(x,t) = \frac{\partial}{\partial x}\left[\eta_{/\!/}(x,t)\left[\frac{1}{\mu_0 a^2 x}\frac{\partial \psi_x}{\partial x} + R_0 j_{bs}(x,t) + R_0 j_{ni}(x,t)\right]\right]$$

$$j_{eff}(x,t) = -\frac{1}{\mu_0 R_0 a^2 x}\frac{\partial \psi_x}{\partial x} \quad \text{or} \quad q(x,t) \doteq \frac{d\phi}{d\psi} = -\frac{B_{\phi_0} a^2 x}{\psi_x}$$

with $\psi_x(0,t) = 0$, $\psi_x(1,t) = f(I_p)$ or $\dot{\psi}(1,t) = f(V_{loop})$ and IC.

A system-identification approach to peripheral modeling [IOP PPCF'07]

- Temperature: grey box modeling & neural network
- Density: averaged scaled profiles
- RF intpus (wave/plasma coupling): identified gaussian distributions
- Time integration: dedicated integration & algebraic operators of integration/differentiation
- Nonlinearity: specific integration as delayed component

$\Rightarrow$ Efficient experimentally tuned model: 3 coupled PDE + wave/particles interaction $\rightarrow$ 1 PDE + identified shapes;

$\Rightarrow$ simulation $\approx$ 20 times faster than real-time!

Experimental results

Lower Hybrid effect: shot TS 35109 - variations in $N_{//}$, constant I_p (0.6 MA) and power input (1.8 MW).

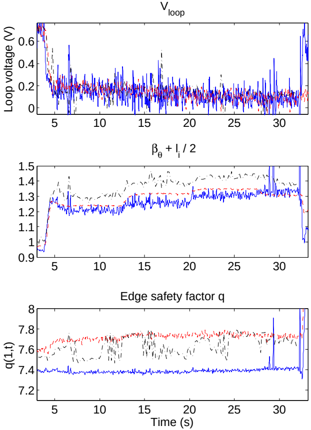

(g) Measured T_e profile

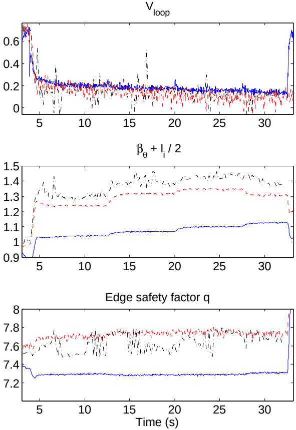

(h) Estimated T_e profile

Figure: ψ_{sim} (—) vs. measurements (– –) and CRONOS (– · –): loop voltage (top), $\beta_\theta + l_i/2$ (middle) and edge safety factor (bottom).

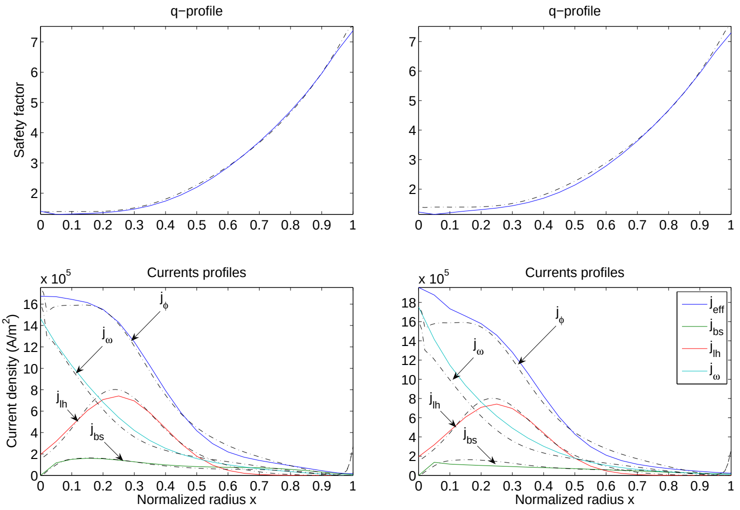

(a) Measured T_e profile

(b) Estimated T_e profile

Figure: ψ_{sim} (—) vs. CRONOS (– · –) at $t = 7\ s$: safety factor (top) and current densities (effective j_ϕ, LH j_{lh}, ohmic j_ω and bootstrap j_{bs}) profiles (bottom).

Feedback control

Comparison of linear lumped approaches ($n_p = 2$, $N = 8$ for control, 22 for simulation) [CDC'10,IFAC'11]

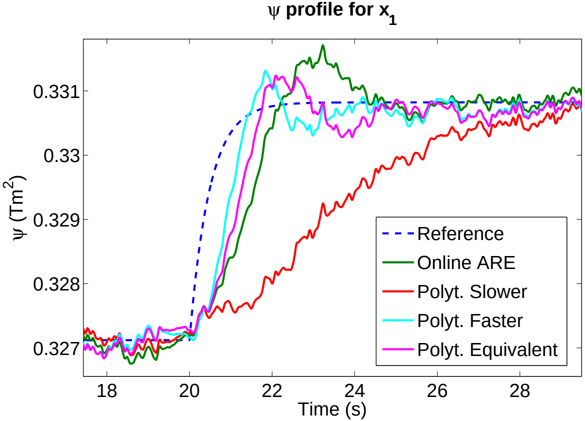

Lyapunov-based PDE control [TAC'12, IOP NF'12] →

Federico's Ph.D. defense at 15:00!

Bootstrap current maximization [CDC'12]

Preliminary conclusions

- Importance of capturing the equilibrium
- Tendency to “flatten” everything between the boundaries
- Performance challenge: overcome sluggishness without triggering peripheral couplings
- Robustness challenge: sensitivity to the distributed parameters and changes in the orders of magnitude

Advective-diffusive transport

$$\frac{\partial \zeta}{\partial t} + \nabla \cdot \mathcal{A}(\zeta, \mathbf{x}, t) + \nabla \mathcal{D}(\nabla \cdot \zeta, \zeta, \mathbf{x}, t) = \mathcal{S}_o(u, \mathbf{x}, t) - \mathcal{S}_i(\zeta, \mathbf{x}, t)$$

$$y = g(\zeta, \mathbf{x}, t)$$

- "Half-opposite" effects of advection and diffusion
- $\mathcal{A}$ typically associated with external forces or unidirectional transport
- $\mathcal{D}$ typically prevents steep gradients
- The transport coefficients set the respective weights

Transport identification from sparse measurements

$$\frac{\partial \zeta}{\partial t} + \nabla \cdot \mathcal{A}(\zeta, \mathbf{x}) + \nabla \mathcal{D}(\nabla \cdot \zeta, \zeta, \mathbf{x}) = \mathcal{S}_o(u, \mathbf{x}, t) - \mathcal{S}_i(\zeta, \mathbf{x})$$

$$y = g(\zeta, \mathbf{x}, t_f)$$

- Need to characterize the I/O map with limited information
- Use physics to describe the qualitative behavior and as much flow quantification as possible
- Use measurements to complete missing signals

Firn inverse modeling and climate change

Trace gas measurements in interstitial air from polar firn:

- reconstruct atmospheric concentration over the last 50 to 100 years
- measures recent anthropogenic impact on atmospheric composition
- i.e. CH_4 transport at NEEM (Greenland)

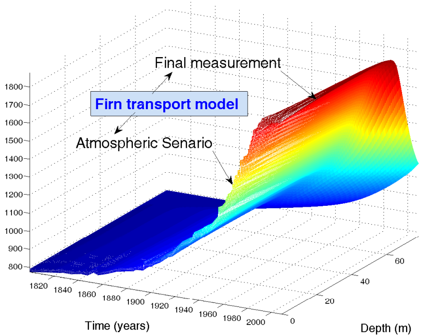

Poromechanics: three interconnected networks [Coussy'03]

Ice lattice, gas connected to the surface (open pores) and gas trapped in bubbles (closed pores):

$$\frac{\partial[\rho_{ice}(1-\epsilon)]}{\partial t} + \nabla[\rho_{ice}(1-\epsilon)\vec{v}] = 0$$

$$\frac{\partial[\rho^o_{gas} f]}{\partial t} + \nabla[\rho^o_{gas} f(\vec{v} + \vec{w}_{gas})] = -\vec{r}^{o\to c}$$

$$\frac{\partial[\rho^c_{gas}(\epsilon - f)]}{\partial t} + \nabla[\rho^c_{gas}(\epsilon - f)\vec{v}] = \vec{r}^{o\to c}$$

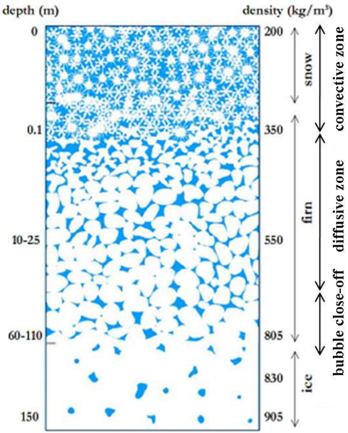

Scheme adapted from [Sowers et al.'92, Lourantou'08].

Trace gas conservation in open pores [Rommelaere & al.'97, ACPD'11]

- Flux driven by advection with air and firn sinking
- Flux driven by mol. diff. due to concentration gradients
- Flux driven by external forces: gravity included with Darcy-like flux
- Sink = particles trapped in bubbles & radioactive decay
- Boundary input: surface concentration
- Results in transport PDE:

$$\frac{\partial}{\partial t}[\rho_\alpha^o f] + \frac{\partial}{\partial z}[\rho_\alpha^o f(v + w_{air})] - \frac{\partial}{\partial z}\left[\mathbf{D}_\alpha\left(\frac{\partial \rho_\alpha^o}{\partial z} - \rho_\alpha^o \frac{\partial \rho_{air}/\partial z}{\rho_{air}} + \mathcal{A}_{ss}\right)\right] = -\rho_\alpha^o(\tau + \lambda)$$

$$\rho_\alpha^o(0,t) = \rho_\alpha^{atm}(t), \qquad \frac{RT}{M_f}\frac{\partial \rho_\alpha^o}{\partial z}(z_f) - \rho_\alpha^o(z_f) = 0$$

with $\mathcal{A}_{ss}$ such that $\partial[\rho_{\alpha,ss}^o f]/\partial t = 0$ at steady state, i.e.

$$\mathcal{A}_{ss} = -\frac{\rho_{\alpha,ss}^o f}{D_\alpha}(w_\alpha - w_{air}) - \rho_{\alpha,ss}^o\left(\frac{\partial \rho_{\alpha,ss}^o/\partial z}{\rho_{\alpha,ss}^o} - \frac{\partial \rho_{air}/\partial z}{\rho_{air}}\right)$$

Validation on isotopic indicators: $\delta^{15}N$ ($\delta^{40}Ar$, $\delta^{86}Kr$)

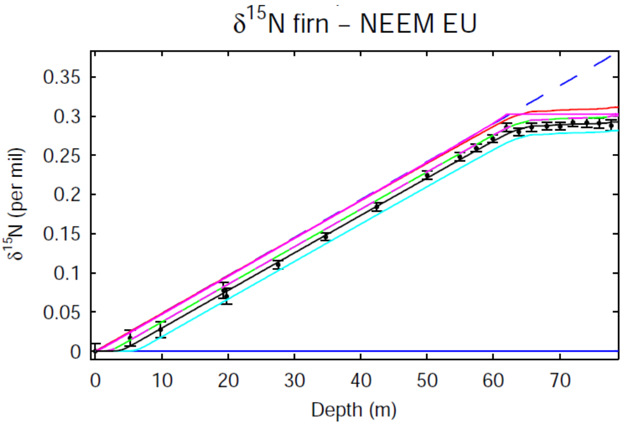

Fick only (blue '—'), QSS (exact in blue '- - -' and gas speed set by air speed in red), QSS with forced LIZ (pink '—'), QSS with $z_{conv} = 4$ m: hydrostatic $\rho^o_{\alpha,ss}$ (green), + max D set by the one in free air + gas-indep term (pink '- - -'), + $z_{conv} = z_{eddy}$ (turquoise), Ref case (black): simplified QSS with $z_{conv} = 4$ m and a max mol. diffu. corrected with the porosity

Advective and diffusive flows in firn

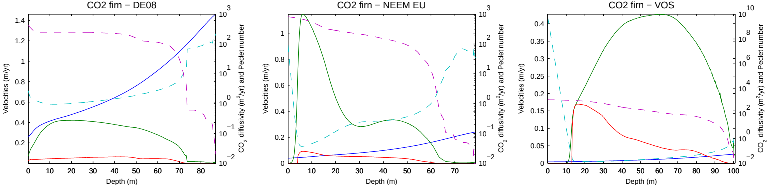

Relative importance of diffusion and advection for CO_2 transport in 1990: velocity due to advection and firn sinking $v + w_{air}$, molecular diffusion $(w_\alpha - w_{air})$, molecular diffusion at steady-state $-(\bar{w}_\alpha - \bar{w}_{air})$, Péclet number and CO_2 diffusivity.

Optimal diffusivity identification [Ieee Med'10]

Final-cost optimization problem with dynamics and inequality constraints

$$\min_D \mathcal{J}(D) = \mathcal{J}_{meas} + \mathcal{J}_{reg}, \text{ under the constraints} \begin{cases} C(\rho, D) = 0 \\ \mathcal{I}(D) < 0 \end{cases}$$

Considering N gas and including the constraints in the cost (*Lagrange* param.):

$$\min_D \mathcal{J}(D) \doteq \sum_{i=1}^{N} [\mathcal{J}_{meas}(\rho_i, \rho_{meas}) + \mathcal{J}_{trans}(C(\rho_i, D))] + \mathcal{J}_{ineq}(D) + \mathcal{J}_{reg}(D)$$

with:

$$\begin{cases} \mathcal{J}_{meas} = \frac{1}{2}\int_0^{z_f} r_i(\rho_{meas} - \rho_i|_{t=t_f})^2 \delta_z \, dz & \text{Measurement cost} \\ \mathcal{J}_{trans} = \int_0^{t_f}\int_0^{z_f} \lambda_i C(\rho_i, D)\, dzdt & \text{Transport constraint} \\ \mathcal{J}_{reg} = \frac{1}{2}\int_0^{z_f} s(z) D^2 \, dz & \text{Regularization function} \end{cases}$$

$\Rightarrow$ Gradient-descent from analytical adjoint computation using the linearized PDE dynamics.

Preliminary results

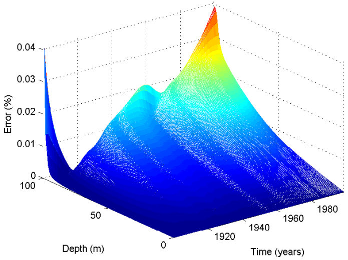

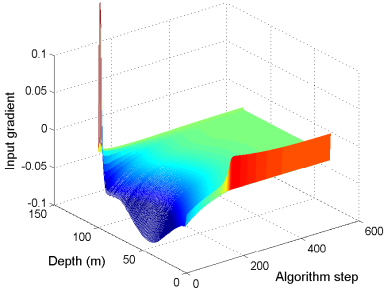

Source reconstruction from (sparse) measurements

$$\frac{\partial \zeta}{\partial t} + \nabla \cdot \mathcal{A}(\zeta, \mathbf{x}(, t)) + \nabla \mathcal{D}(\nabla \cdot \zeta, \zeta, \mathbf{x}(, t))$$
$$= \mathcal{S}_o(u, \mathbf{x}, t) - \mathcal{S}_i(\zeta, \mathbf{x})$$
$$y = g(\zeta, \mathbf{x}, t_f(, t))$$

- Use the identified transport to determine the “optimal” input
- Under-constrained problem: need for regularization
- How to estimate the information content?

A "deconvolution" approach for atmospheric scenario reconstruction [Rommelaere et al., JGR, 1997]

- Green function = impulse response of the firn ⇒ age probabilities

$$\rho_{firn}(z, t_f) = G(z, t) * \rho_{atm}(t) \qquad \text{convolution}$$

- Deconvolution:

$$\begin{aligned} \epsilon(z) &= G(z, t)\rho_{atm}(t) - \rho_{firn}(z, t_f) \\ \rho^*_{atm}(t) &= \arg\min_{\rho_{atm}} \left[\epsilon^T (diag\{1/\sigma^2_{mes}(z)\})\epsilon + \kappa^2 \rho^T_{atm} R \rho_{atm}\right] \end{aligned}$$

- Under-constrained pb ⇒ add extra information with rugosity characteristic matrix $R > 0$ (i.e. d^2/dt^2) + κ.
- 2 parameters largely control model behavior: κ (rugosity factor) and $\sigma^2_{mes}(z)$

⇒ Extension to a multi-site analysis:
$G(z, t) \rightarrow [G_1^T \; G_2^T \; \dots G_{N_{sites}}^T]^T$

Reconstruct CO isotopic ratios history and CO budget

[Wang et al., ACP'12]

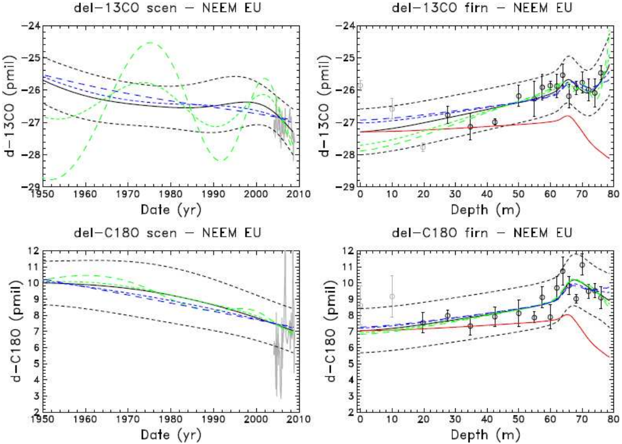

"Fossil fuel CO emissions decreased as a result of the implementation of catalytic converters and the relative growth of diesel engines, in spite of the global vehicle fleet size having grown several fold over the same time period"

Finally solving the tokamak n_e source id

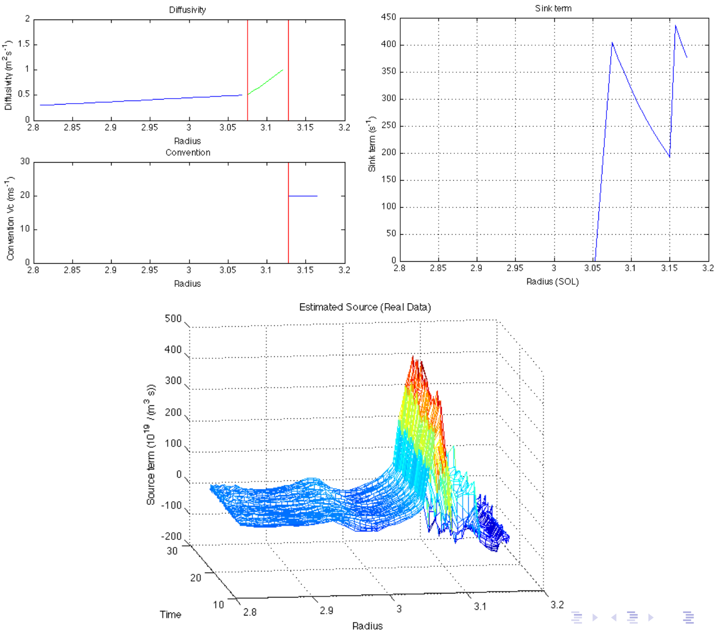

Conclusions

- A global methodology is hard to define
- General trends from advective versus diffusive behavior
- Model toward solving the control/identification problem
- i.e. time-delay approaches (Lyapunov-Krasovskii) versus adjoint-based optimization or Lyapunov functionals
- Modeling is an art . . . which necessitates a broad scientific knowledge!

Special thanks

- Benjamin BRADU
- Corentin BRIAT
- Federico BRIBIESCA-ARGOMEDO
- Felipe CASTILLO BUENAVENTURA
- Sumanth CHINTHALA
- Aditya GAHLAWAT
- Xiao Dong LI
- Sarah MECHHOUD
- Erik OLOFSSON
- Pangun PARK
- Maria RIVAS
- ...